Springer Series in
MATERIALS SCIENCE 100

Springer Series in

MATERIALS SCIENCE

Editors: R. Hull R. M. Osgood, Jr. J. Parisi H. Warlimont

The Springer Series in Materials Science covers the complete spectrum of materials physics, including fundamental principles, physical properties, materials theory and design. Recognizing the increasing importance of materials science in future device technologies, the book titles in this series reflect the state-of-the-art in understanding and controlling the structure and properties of all important classes of materials.

88 **Introduction to Wave Scattering, Localization and Mesoscopic Phenomena**
By P. Sheng

89 **Magneto-Science**
Magnetic Field Effects on Materials: Fundamentals and Applications
Editors: M. Yamaguchi and Y. Tanimoto

90 **Internal Friction in Metallic Materials**
A Handbook
By M.S. Blanter, I.S. Golovin, H. Neuhäuser, and H.-R. Sinning

91 **Time-dependent Mechanical Properties of Solid Bodies**
By W. Gräfe

92 **Solder Joint Technology**
Materials, Properties, and Reliability
By K.-N. Tu

93 **Materials for Tomorrow**
Theory, Experiments and Modelling
Editors: S. Gemming, M. Schreiber and J.-B. Suck

94 **Magnetic Nanostructures**
Editors: B. Aktas, L. Tagirov, and F. Mikailov

95 **Nanocrystals and Their Mesoscopic Organization**
By C.N.R. Rao, P.J. Thomas and G.U. Kulkarni

96 **GaN Electronics**
By R. Quay

97 **Multifunctional Barriers for Flexible Structure**
Textile, Leather and Paper
Editors: S. Duquesne, C. Magniez, and G. Camino

98 **Physics of Negative Refraction and Negative Index Materials**
Optical and Electronic Aspects and Diversified Approaches
Editors: C.M. Krowne and Y. Zhang

99 **Self-Organized Morphology in Nanostructured Materials**
Editors: K. Al-Shamery, S.C. Müller, and J. Parisi

100 **Self Healing Materials**
An Alternative Approach to 20 Centuries of Materials Science
Editor: S. van der Zwaag

101 **New Organic Nanostructures for Next Generation Devices**
Editors: K. Al-Shamery, H.-G. Rubahn, and H. Sitter

102 **Photonic Crystal Fibers**
Properties and Applications
By F. Poli, A. Cucinotta, and S. Selleri

103 **Polarons in Advanced Materials**
Editor: A.S. Alexandrov

Volumes 40–87 are listed at the end of the book.

S. van der Zwaag

Self Healing Materials

With 242 Figures

Springer

S. van der Zwaag
Technical University
Delft, The Netherlands

Series Editors:

Professor Robert Hull
University of Virginia
Dept. of Materials Science and Engineering
Thornton Hall
Charlottesville, VA 22903-2442, USA

Professor R. M. Osgood, Jr.
Microelectronics Science Laboratory
Department of Electrical Engineering
Columbia University
Seeley W. Mudd Building
New York, NY 10027, USA

Professor Jürgen Parisi
Universität Oldenburg, Fachbereich Physik
Abt. Energie- und Halbleiterforschung
Carl-von-Ossietzky-Strasse 9–11
26129 Oldenburg, Germany

Professor Hans Warlimont
Institut für Festkörper-
und Werkstofforschung,
Helmholtzstrasse 20
01069 Dresden, Germany

A C.I.P. Catalogue record for this book is available from the Library of Congress

ISSN 0933-033x

ISBN 978-1-4020-6249-0 (HB)

ISBN 978-1-4020-6250-6 (e-book)

Published by Springer,
P.O. Box 17, 3300 AA Dordrecht, The Netherlands

www.springer.com

Foreword

"As a general principle natural selection is continually trying to economise every part of the organisation." That was Charles Darwin, writing over 100 years ago about efficiency in nature. Natural materials are remarkably efficient. By efficient we mean that they fulfil the complex requirements posed by the way plants and animals function, and that they do so using as little material as possible. Many of these requirements are mechanical in nature: the need to support static and dynamic loads created by the mass of the organism or by wind loading, the need to store and release elastic energy, the need to flex through large angles, the need to resist buckling and fracture, and to survive damage. Few optimisation algorithms have been more successful than that of "survival of the fittest". The structural materials of nature exemplify this optimisation; even today, few man-made materials do better than those of nature in the function that they fill. And of all the remarkable properties of natural materials, one is truly exceptional – that of the ability for self-repair.

One recurring goal of material development has been to emulate the materials of nature. Among these, the most illusive is that of self-repair. In approaching this it is well to be aware of the nature of the differences that separate the structural materials of man and those of nature. The table itemises some of these: the great differences in chemistry, in mode of synthesis, in structure, and above all in the ability of natural materials for continuous adaptation and replacement, damage-sensing and repair. Man-made materials that achieve it are few: the self healing properties of the lime cement used by the early Roman Empire, the healing of oxide films that provide the corrosion resistance of aluminium, titanium, and stainless steel, the recrystallisation of metals to restore the pre-deformed properties, and a few others.

A comparison of features of man-made and natural structural materials.

Man-made Structural Materials	Structural Materials of Nature
Based on the entire periodic table	Based on few elements (C, N, O, Ca, Si, etc.)
Thermo-chemistry (high temperature) processing	Ambient temperature processing
Fast production rate	Slow growth rate
Largely monolithic or simple composite structures	Complex, hierarchical structures
Unchanging structure once fabricated	Continuous replacement and renewal
No ability to adapt to change of environment	Ability to adapt evolving environment
No capacity, in general, for self-repair	Ability to sense damage and self-repair
Thus: requiring "worst-case" design with additional safety factor	Thus: allowing optimal design to match current conditions without penalty of large safety factor

The contributors' initiative to bring together all these interesting concepts and early attempts at developing, describing, and even modelling self healing in materials is visionary and ambitious, and one that takes a broad stance and is the first of its kind. The spread of self healing strategies and of material systems to which they might be applied is broad, including polymers, composites, ceramics, metals, coatings, adhesives, and – significantly – the materials that inspired it all, those of nature. The editor and the contributors are to be congratulated on creating an impressive overture and opening movement to what is a sector of materials research and development with enormous potential.

Mike Ashby
Engineering Department
University of Cambridge
May 2007

Preface

This book *Self healing materials: an alternative to 20 centuries of materials science* is the 100th textbook in the Springer Series on Materials Science and opens the door to a new era in materials science: *self healing materials*.

Over the last 20 centuries the properties of structural materials at our disposal have improved tremendously in every aspect. The early improvements were due to a slow trial and error process, appropriately called "black magic" at the time, guided by just the appraisal of the final material, or more importantly the resulting product performance. The development took place without real knowledge of the material itself, or of the internal changes taking place during materials processing. In the nineteenth, and in particular, in the twentieth centuries, however, the pace of material development accelerated greatly. Two major factors played a role in this development: the notion of a microstructure in combination with physicochemical techniques to quantify it, and the availability of (semiempirical) models linking the microstructure to the final material properties and vice versa. Both factors led to a real acceleration of material development and today material properties can be tuned precisely, and to very high levels, sometimes even approaching the theoretical limits.

With hindsight, all strategies to improve the strength and reliability of materials developed over the last 20 centuries are ultimately based on the paradigm of *damage prevention*, i.e. the materials are designed and prepared in such a way that the formation and extension of damage as a function of load and/or time is postponed as much as possible. Damage is defined here as the presence of micro- or macroscopic cracks not being present initially. Characteristic for the current materials, developed under the damage prevention paradigm, is that the levels of damage in a material can either remain constant or increase, but will never go down spontaneously.

In recent years, however, it has been realized that an alternative strategy can be followed to make materials effectively stronger and more reliable, and that is by *damage management*, i.e. materials have a built-in capability to repair the damage incurred during use. Cracks are allowed to form, but the material itself is capable of repairing the crack and restoring the functionality of the material. Such damage management is encountered in natural materials such as, for example, skin tissue and bone structures. Although the mechanical properties of skin and bone are inferior to those of man-made polymers and ceramics, their ability to repair or heal damage (given the right healing conditions) results in a "lifelong" performance. Of course, given the huge difference in microstructure and chemical species involved, the mechanisms of

healing in natural materials cannot be copied exactly. Some forms of self healing have been already been demonstrated, but it is anticipated that many more self healing mechanisms can and will be found with the progression of this novel branch of materials science.

This book aims at bringing together for the first time a more or less complete overview of the developments in the field of self healing materials, not just focused on one material class but covering all important man-made material classes, polymers, composites, metals, concrete, and bituminous materials. To put our human efforts in a wider context, two chapters on skin and bone healing are added as well. As is not uncommon in the field of material science, most of the chapters deal with experimental research, but several chapters also present early theoretical concepts towards modeling self healing phenomena, and are aimed at assisting material developers in creating self healing materials more quickly and more efficiently. As the editor of this first book on self healing materials I am very grateful for all the experts who made their valuable contribution to this book.

The book in its current form should be attractive to the entire community of material scientists working on both structural and functional materials. In addition, the level of subject-specific knowledge is kept to such a level that the book would be very suitable as a textbook in courses on self healing materials at both the undergraduate and graduate level. The CD, which goes with the book, contains the proceedings of the first international conference on self healing materials (18–20 April 2007, Noordwijk, the Netherlands), adding even more aspects of recent works in the field of self healing materials.

Finally, it must be emphasized that the book is written at a relatively early stage of development of the field and that a variety of challenges need yet to be met before we will see a wide application of such materials in daily life, a topic, which will definitely be included in the next edition of this book. The authors, however, are confident that in time we will be able to present a new edition of this book in which commercially and technologically successful applications of self healing materials are presented as well.

Contents

Self Healing in Concrete Materials

Victor C. Li and Enhua Yang

Department of Civil and Environmental Engineering, University of Michigan, Ann Arbor, USA

1 Introduction

1.1 Background

The phenomenon of self healing in concrete has been known for many years. It has been observed that some cracks in old concrete structures are lined with white crystalline material suggesting the ability of concrete to seal the cracks with chemical products by itself, perhaps with the aid of rainwater and carbon dioxide in air. Later, a number of researchers [1, 2] in the study of water flow through cracked concrete under a hydraulic gradient, noted a gradual reduction of permeability over time, again suggesting the ability of the cracked concrete to self-seal itself and slow the rate of water flow. The main cause of self-sealing was attributed to the formation of calcium carbonate, a result of reaction between unhydrated cement and carbon dioxide dissolved in water [1]. Thus, under limited conditions, the phenomenon of self-sealing in concrete is well established. Self-sealing is important to watertight structures and to prolonging service life of infrastructure.

In recent years, there is increasing interest in the phenomenon of mechanical property recovery in self healed concrete materials. For example, the resonance frequency of an ultra high-performance concrete damaged by freeze–thaw actions [3], and the stiffness of pre-cracked specimens [4] were demonstrated to recover after water immersion. In another investigation, the recovery of flexural strength was observed in pre-cracked concrete beams subjected to compressive loading at early age [5]. In these studies, self healing was associated with continued hydration of cement within the cracks. As in previous permeability studies, the width of the concrete cracks, found to be critical for self healing to take place, was artificially limited using feedback-controlled equipment and/or by the application of a compressive load to close the preformed crack. These experiments confirm that self healing in the mechanical sense can be attained in concrete materials.

Deliberate engineering of self healing in concrete was stimulated by the pioneering research of White and coworkers [6, 7] who investigated self healing of polymeric material using encapsulated chemicals. A number of experiments were conducted on methods of encapsulation, sensing, and actuation to release the encapsulated chemicals [8–12] into concrete cracks. For example, Li et al. [10] demonstrated that air-curing polymers released into a crack could lead to a recovery of the composite elastic modulus. The chemical release was actuated by the very action of crack formation

S. van der Zwaag (ed.), *Self Healing Materials. An Alternative Approach to 20 Centuries of Materials Science*, 161–193.

in the concrete, which results in breaking of the embedded brittle hollow glass fibers containing the polymer. Thus, the healing action took place where it was needed. Another approach, taken by Nishiwaki et al. [13], utilized a repair agent encapsulated in a film pipe that melts under heating. A heating device was also embedded to provide heat to the film pipe at the cracked location when an electric current is externally supplied. Yet another approach, suggested by the experiments of Bang et al. [14] and Rodriguez-Navarro et al. [15], used injected microorganisms to induce calcite precipitation in a concrete crack. These novel concepts represent creative pathways to artificially inducing the highly desirable self healing in concrete materials.

From a practical implementation viewpoint, autogenous self healing is most attractive. Compared to other engineering materials, concrete is unique in that it intrinsically contains micro-reservoirs of unhydrated cement particles widely dispersed and available for self healing. In most concrete and particularly in those with a low water/cement ratio, the amount of unhydrated cement is expected to be as much as 25% or higher. These unhydrated cement particles are known to be long lasting in time. Autogenous self healing is also economical, when compared with chemical encapsulation or other approaches that have been suggested. As indicated above, the phenomenon of autogenous self healing has been demonstrated to be effective in transport and mechanical properties recovery. Unfortunately, the reliability and repeatability of autogenous self healing is unknown. The quality of self healing is also rarely studied, and could be a concern, especially if weak calcite is dependent upon for mechanical strength recovery. Perhaps the most serious challenge to autogenous healing is its known dependence on tight crack width (CW), likely less than 50 μm, which is very difficult to achieve in a consistent manner for concrete in the field. In practice, concrete CW is dependent on steel reinforcement. However, the reliability of CW control using steel reinforcement has been called into question in recent years. The latest version of the ACI-318 code has all together eliminated the specification of allowable CW. Thus, a number of serious material engineering challenges await autogenous healing before this phenomenon can be relied upon in concrete structures exposed to the natural environment.

To create practical concrete material with effective autogenous self healing functionality, the following six attributes are considered particularly important. For convenience, we label a material with all these six attributes of autogenous self healing as "robust":

- *Pervasiveness*: Ready for activation when and where needed (i.e. at the crack when cracking occurs)
- *Stability*: Remain active over the service life of a structure that may span decades
- *Economics*: Economically feasible for the highly cost-sensitive construction industry in which large volumes of materials are used daily
- *Reliability*: Consistent self healing in a broad range of typical concrete structure environments
- *Quality*: Recovered transport and mechanical properties as good as pre-damage level

- *Repeatability*: Ability to self-repair for multiple damage events

In this chapter, we review recent experimental findings of the autogenous recovery of mechanical properties and transport properties in a specially designed cementitious material known as Engineered Cementitious Composite, or ECC. ECC has been deliberately engineered to possess self-controlled CW that does not depend on steel reinforcement or structural dimensions [16]. Instead, the fibers used in ECC are tailored [17] to work with a mortar matrix in order to suppress localized brittle fracture in favor of distributed microcrack damage, even when the composite is tensioned to several percent strain. ECC with CW as low as 30 μm have been made. The ability of ECC to maintain extremely tight CW in the field has been confirmed in a bridge deck patch repair [18] and in an earth-retaining wall overlay [19].

The deliberately pre-cracked ECC specimens were exposed to various commonly encountered environments, including water permeation and submersion, wetting and drying cycles, and chloride ponding. The mechanical properties studied include dynamic modulus, tensile stiffness, strength, and ductility. The transport properties studied include water permeability and chloride diffusivity.

The rest of this introduction is devoted to a concise review of the conditions required for reliable autogenous self healing, based on published literature (section 1.2). Further background information on ECC, with emphasis on tight CW control, is provided in section 1.3.

1.2 Review of Conditions for Reliable Autogenous Self Healing

Previous researchers have engaged in limited studies in the phenomenon of concrete self healing, the formation of self healing products, and the necessary conditions to experience self healing in concrete materials. These studies have resulted in identifying three general criteria which are critical to exhibit reliable autogenous self healing – presence of specific chemical species, exposure to various environmental conditions, and small CW. These are summarized below. In some instances these findings are contradictory, as in the case of maximum allowable CW in which some specify maximum CWs of 10 μm, while others specify 300 μm to exhibit self healing in various environmental conditions:

- Essential environmental exposure – water (submerged) [20, 21], environmental pH [22, 23], wet–dry cycles (capillary suction) [24], temperature above 80° C [2], temperature above 300° C [25]
- Essential chemical species – bicarbonate ions (HCO_3^-) [1, 23, 26], carbonate ions (CO_3^{2-}) [1, 23, 26], free calcium ions (Ca^{2+}) [1, 23, 26], unhydrated cement (C_3A) [25, 27], free chloride ions (Cl^-) [28–30]
- Maximum CW −5–10 μm [31], 53 μm [32], 100 μm [2], 200 μm [1], 205 μm [33], 300 μm [20]

While the individual findings may differ, trends within these studies are clear. First, self healing can occur in a variety of environmental conditions ranging from underwater to cyclic wet–dry exposures. These conditions are readily available for many infrastructure types. Second, adequate concentrations of certain critical chemical species are essential to exhibit self healing mechanisms. This too, is readily available due to the chemical make up of cementitious materials and incomplete hydration, as well as the presence of CO_2 in air and NaCl in seawater and deicing salt. Finally, and potentially most important, is the requirement for tight CWs below roughly 200 μm, possibly 50 μm. This condition is difficult to achieve consistently, and explains why reliable formation of self healing products in most concrete structures has not been realized. This set of material physical and chemical properties, and exposure conditions, may serve as a reference base towards systematic design of robust self healing concrete.

Very little work has been carried out in determining the quality of self healing and its repeatability.

1.3 ECC Engineered for Tight Crack Width Control

In recent years, fiber-reinforced cement-based composites optimized for ultra high-tensile ductility while minimizing the amount of fibers have been designed based on micromechanics design tools [34]. Such materials, defined as ECC, attain desirable inelastic deformation mechanisms through ingredients tailored to interact synergistically under load, rather than relying on high-fiber content. Specifically, the type, size, and amount of ingredients of ECC, including cement, fiber, sand, fly ash, water, and other chemical additives commonly used in fiber-reinforced cementitious composites are determined from micromechanics such that the composite "plastically yields" under excessive loading through controlled microcracking while suppressing brittle fracture localization. Table 1 gives an example of composition of ECC. The volume fraction of fiber is 2%. ASTM Type I portland cement and low-calcium ASTM class F fly ash are used. Large aggregates are excluded in ECC mix design, and only fine sand is incorporated. The silica sand has a maximum grain size of 250 μm and an average size of 110 μm. The PVA fiber has a diameter of 39 μm, a length of 12 mm, and overall Young's modulus of 25.8 GPa. The apparent fiber strength when embedded in cementitious matrix is 900 MPa. The fiber surface is treated with a proprietary oil coating of 1.2% by weight.

Figure 1 shows an example of the uniaxial tensile stress–strain curve of ECC that exhibits a "yielding" behavior similar to that of ductile metals. The tensile strain

Table 1 Mix proportions of a PVA-ECC (kg/m^3)

Cement	Sand	Class F Fly Ash	Water	Superplasticizer	PVA Fiber
583	467	700	298	19	26

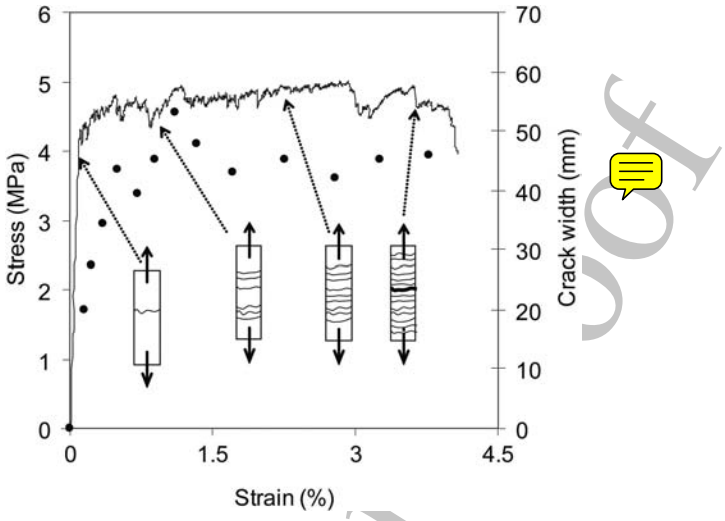

Fig. 1 Typical tensile stress–strain curve of ECC

capacity of ECC is 400–500 times that of normal concrete and the fracture toughness of ECC is similar to that of aluminum alloys [35]. Furthermore, the material remains ductile even when subjected to high shear stress [36]. The compressive strength of ECC ranges from 40–80 MPa depending on mix composition, the high end similar to that of high-strength concrete.

During tensile deformation up to about 1% strain, microcracks are formed in the specimen with CW increasing from zero to a steady-state value (about 50 μm shown in Figure 1). When the material is subjected to additional straining, more microcracks are formed, but the CW remains more or less constant. This steady-state CW is an intrinsic property of ECC and depends only on the fiber and fiber/matrix interface properties [37] which are deliberately tailored. It does not depend on the structural size or the amount of steel reinforcement. The ability of the material to exhibit tight CW control in the field, beyond laboratory conditions, is important in realizing robust self healing in actual structures. The relation between reliable self healing and tight CW is emphasized in this chapter.

2 Self healing in ECC

The chemical makeup and physical characteristics, inherent tight CW control in particular, of ECC makes self healing behavior in ECC material prevail under proper environmental conditions. This section summarizes recent laboratory test results on the self healing behavior in ECC material.

2.1 Self Healing Examination Methods

In the published literature, a number of techniques have been used to detect self healing and/or to quantify the quality of self healing in cementitious materials. Permeability test and acoustic emission technology are two common such techniques [1, 2, 28–31,33, 38–41]. In many studies, a falling head or constant head test is used to examine the extent of self healing by monitoring the flow rate or quantity of water passing through the cracked specimens. The change in the coefficient of permeability of concrete with respect to time is used to measure the amount of self healing which has occurred. Typically, a gradual reduction in this coefficient is used to infer self healing taking place in the specimen. This approach is restricted to describing self healing of transport property through permeation, and also requires that the promotion of self healing derive from fluid (typically water which may carry dissolved CO_2) flow through the crack. Formation of chemical products such as calcite in the crack has been cited as a reason for increase of sealing function over time [1, 2, 28, 29, 38]. The permeability test is typically used to examine self healing of a single crack although it can be applied to water permeability through multiple cracks.

Acoustic emission technology based on ultrasonic pulse velocity (UPV) measurements has also been used to assess crack healing. Although UPV measurement can detect the occurrence of crack healing, it has been shown that this method cannot accurately determine the extent of crack healing [33]. Resonant frequency or dynamic modulus measurements [30, 31, 42, 43] and pulse echo technique [25, 33] have also been used by a number of researchers to quantify the self healing process. Recently, one-sided stress wave transmission measurements were used to characterize the process of self healing. Based on the experimental observation; however, this transmission measurement is unable to clearly distinguish among CWs above 100 μm [33]. The advantage of these techniques is that they can be conducted relatively fast. However, these methods cannot explicitly differentiate between the nature of self healing – recovery of mechanical and/or transport properties – taken place. Material bulk properties are inferred from the test data.

In order to develop a more comprehensive understanding of self healing in ECC, four methods have been used in examining its self healing behavior. The dynamic modulus measurements provide a quick means to assess the presence of self healing. The uniaxial tension test is used to determine self healing of mechanical properties. Water permeability is used to examine the recovery of transport property through permeation. Surface chemical analysis (XEDS) and environmental scanning electron microscopy (ESEM) are used to analyze the chemical composition and morphology of self healing product. Each of these test methods is described in more detail below. Together, they show unequivocally the presence of self healing in ECC in both the transport sense and in the mechanical sense.

2.1.1 Dynamic Modulus Measurements

The material dynamic modulus measurement based on ASTM C215 (Standard Test Method for Fundamental Transverse, Longitudinal, and Torsional Resonant Frequency of Concrete Specimens) appears to be a particularly promising technique to monitor the extent and rate of autogenous healing. This test method (ASTM C215), which relies on changes in resonant frequency, has proven a good gauge of material degradation due to freeze thaw damage and is specifically referenced within ASTM C666 for freeze thaw evaluation. Rather than quantifying damage; however, it has been adapted to measure the extent and rate of self healing in cracked concrete [43], when healing is seen as a reduction in material damage.

Prior to using resonant frequency as an accurate measure of "healing" within a cracked ECC specimen, it is essential to verify it as a valid measurement of internal damage/healing. Therefore, a series of ECC specimens measuring $230 \times 76 \times 13$ mm were prepared and subjected to varying levels of strain deformation ranging from 0% to 4% (i.e. different damage level) under uniaxial tension (see section 2.1.2) at 28 days. After unloading, the resonant frequency of each cracked specimen was determined.

From this series of tests, a relationship between tensile strain (i.e. damage) and change in resonant frequency was determined. Further, this relation extends to the number of cracks within a specimen versus resonant frequency. These relations are shown in Figure 2 and b, respectively. The resonant frequency has been normalized by that at zero strain, i.e. the resonant frequency measured with the virgin ECC without preloading. These figures show a distinct bilinear relationship between the resonant frequency and the tensile strain deformation or number of cracks. Below approximately 1% strain, a sharp drop in resonant frequency with strain/crack number can be seen, while above 1% strain this trend softens. The bilinear relationship may be attributed to the increase in number and CW (from 0 μm to 50 μm) of the multiple-microcracks at low-strain level, while only increase in crack number at steady state CW (50 μm) has been observed after about 1% strain. These results indicate that a change of resonant frequency can be used to quantify the degree of damage (i.e. tensile strain beyond the first crack) to which an ECC specimen has been subjected. Therefore, this technique should prove useful in quantifying both the rate (with respect to cycles of exposures, see section 2.2) and extent of self healing, or "negative damage", within cracked ECC specimens.

2.1.2 Uniaxial Tensile Test

Unlike conventional concrete material, tensile strain-hardening behavior represents one of the most important features of ECC material. To assess the quality of self healing in such materials, the magnitude of recovered mechanical properties were measured under uniaxial tensile loading. First, deliberate damage was introduced by tensioning a coupon specimen to predetermined strain levels followed by unloading.

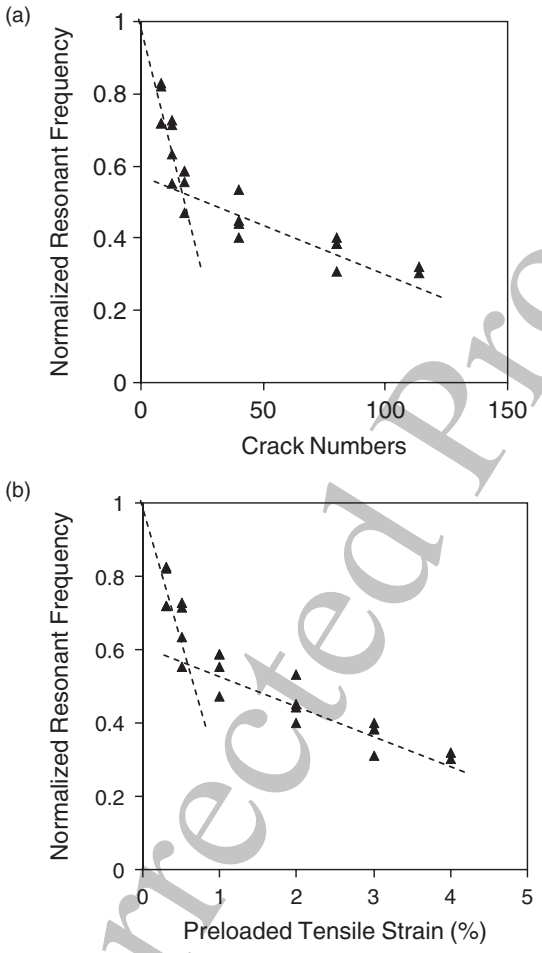

Fig. 2 Resonant frequency as an indicator for internal damage: (**a**) Resonant frequency as a function of preloaded tensile strain; (**b**) Resonant frequency as a function of crack numbers

After exposure to a healing environment, the specimen is then reloaded in direct tension to analyze the recovery magnitude of tensile strength, stiffness and strain capacity in ECC as shown in Figure 3. These properties were then compared with those measured before damage (in the case of elastic stiffness) and with those after damage but before self healing. A servohydraulic testing system was used in displacement control mode to conduct the tensile test. The loading rate used was 0.0025 mm/s to simulate a quasi-static loading condition. Aluminum plates were glued both sides at the ends of coupon specimens to facilitate gripping. Two external linear variable displacement transducers were attached to the specimen to measure the specimen deformation.

Fig. 3 Setup of the uniaxial tensile test

2.1.3 Water Permeability Test

Water permeability test was carried out to measure the transport property, permeability coefficient, of material either virgin (uncracked), preloaded (cracked/damaged), or rehealed specimen. To conduct permeability test, two experimental setups were used. A falling head test was used for specimens with a low permeability, while a constant head test was used for specimens (such as those with large CW) with a permeability too high to practically use the falling head test. These two setups are shown schematically in Figure 4a and b, respectively. The falling head and constant head permeability test setups have been adapted from Wang et al. [40] and Cernica [44].

The permeability of specimens in the falling head test can be determined using Equation 1 [44], while the permeability of specimens in the constant head test can be determined using Equation 2 [44].

$$k = \frac{a \cdot L}{A \cdot t_f} \left(\frac{h_0}{h_f} \right) \tag{1}$$

$$k = \frac{V \cdot L}{A \cdot h_0 \cdot t_f} \tag{2}$$

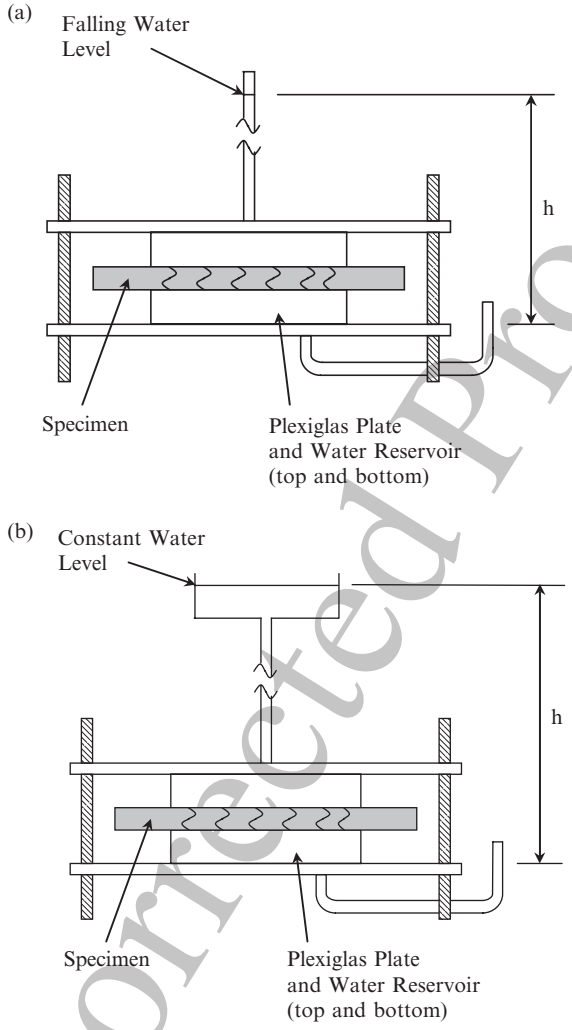

Fig. 4 Permeability test setups: (**a**) Falling head permeability test setup; (**b**) Constant head permeability test setup

where k is the coefficient of permeability, a is the cross-sectional area of the standpipe, L is the specimen thickness in the direction of flow, A is the cross-sectional area subject to flow, t_f is the test duration, h_0 is the initial hydraulic head, h_f is the final hydraulic head, and V is the volume of liquid passed through the specimen during the test.

2.1.4 Microscopic Observation and Analysis

The quality of healing is likely influenced by the type of self healing products formed inside the crack. Analyses of these products were conducted using ESEM and x-ray energy dispersive spectroscopy (XEDS) techniques. The crystalline and chemical properties of self healing products were determined. These techniques are particularly useful in verifying the chemical makeup of self healing compounds, essential in identifying the chemical precursors to self healing and ensuring their presence within the composite.

2.2 Environmental Conditioning

As described in the previous section (section 1.2), the robustness of self healing should be examined under a variety of environmental exposures typically experienced by concrete infrastructure systems. In the investigation of self healing of ECC, various environmental conditioning regimes have been adopted. These include cyclic wetting and drying, conditioning temperature, and immersion in water or chloride solution. Specifics of the conditioning regimes are summarized below:

- CR1 (water/air cycle) subjected pre-cracked ECC specimens to submersion in water at 20°C for 24 h and drying in laboratory air at 21°C ± 1°C, 50% ± 5% RH for 24 h, during which no temperature effects are considered. This regime is used to simulate cyclic outdoor environments such as rainy days and unclouded days.
- CR2 (water/hot air cycle) consisted of submersion of pre-cracked ECC specimens in water at 20°C for 24 h, oven drying at 55°C for 22 h, and cooling in laboratory air at 21°C ± 1°C, 50% ± 5% RH for 2 h. This regime is used to simulate cyclic outdoor environments such as rainy days followed by sunshine and high temperatures in summer.
- CR3 (water permeation) consisted of continuous permeation through cracked ECC specimen in water at 20°C till the predetermined testing ages. This regime is used to simulate environmental conditions of infrastructure in continuous contact with water with a hydraulic gradient, such as water tank, pipelines, and irrigation channels.
- CR4 (chloride solution submersion) considered direct exposure of pre-cracked ECC specimens to a solution with high chloride content. This regime is used to simulate the exposure to deicing salt in transportation infrastructure or parking structures, or in concrete containers of solutions with high salt content.
- CR5 (water submersion) consisted of submersion in water at 20°C till the predetermined testing ages. This regime is used to simulate ECC in some underwater structures.

2.3 *Effect of Crack Width on Self Healing*

To examine the effect of CW on self healing, mortar coupon specimens measuring 230 × 76 × 13 mm reinforced with a small amount (0.5vol.%) polyvinyl alcohol (PVA) fiber were prepared. These specimens were deliberately made to exhibit tension-softening response typical of normal fiber reinforced concrete so that a single crack of controlled CW can be introduced. Each specimen was first preloaded under uniaxial tension to produce a single crack with a CW between 0 μm and 300 μm. Negligible closing of the crack was detected upon unloading. After unloading, the specimen was exposed to ten wetting and drying cycles (CR1). Resonant frequency was measured after preloading and 10 wetting and drying cycles (CR1) to monitor the extent of self healing of specimen with different CWs.

Figure 5 shows the resonant frequency of specimens before and after wet–dry cycles as a function of CW. The *y*-axis gives the resonant frequency of preloaded specimens before and after the prescribed wet–dry conditioning, normalized to the resonant frequency of uncracked (virgin) material. Therefore, 100% represents a total recovery of the resonant frequency. It is expected that further hydration and moisture content changes during the specimen conditioning regimes may contribute to some fraction of the resonant frequency recovery. To account for this, the averaged resonant frequency of virgin uncracked specimens under the same 10 cyclic conditioning regimes (10 cycles of CR1) was used in the normalization. Each data point represents the average of three test results. As seen in Figure 5, the resonant frequency of specimens after 10 cyclic wet–dry exposures can recover up to 100% of the uncracked value provided that CWs are kept below 50 μm. With an increase of CW; however,

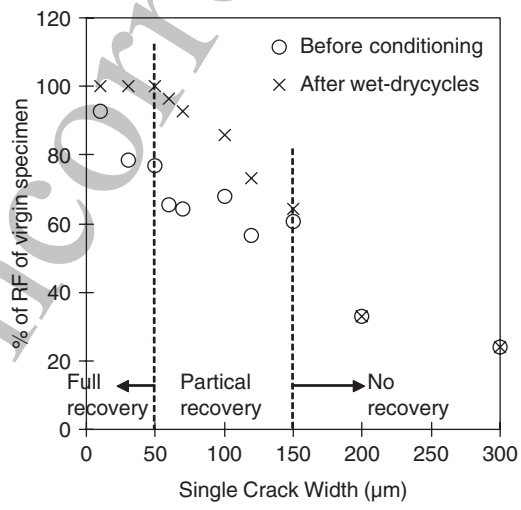

Fig. 5 Recovery of resonant frequency (RF) as a function of crack width

the degree of material damage indicated by the drop in resonant frequency increases and the extent of self healing diminishes. When the CW exceeds 150 μm, the specimen resonant frequency remains unchanged after undergoing the wet–dry cycle conditioning, signifying the difficulty of repairing microstructural damage within these cracked materials. Therefore, maintaining a CW below 150 μm, and preferably below 50 μm, is critical to enable the process of self healing.

Along with the resonant frequency monitoring, permeability tests were conducted on those specimens after 10 wet–dry cycles. Table 2 summarizes the permeability coefficient of preloaded specimen after 10 cyclic conditioning exposures as a function of CW. Although it is known [45] that self healing can occur during the very act of performing a permeability test, the data shown here were initial values so that permeability changes during the test were deliberately excluded. Thus any self healing detected here were due to the wet–dry cycle exposures. From Figure 6, it can be seen that after conditioning, the permeability of specimens with CWs below 50 μm is essentially identical to that of virgin uncracked specimens, which represents a full recovery of transport property, permeability. With increasing CW, the permeability increases exponentially.

AQ: Table 2 cited in text but Table not provided. Please check.

The resonant frequency measurements and the permeability measurements together suggest that complete and autogenous self healing within cement-based materials in both mechanical and transport properties can be achieved, provided that damage must be restricted to very tight CWs, below 50 μm. This extremely tight CW is difficult to attain reliably in most concrete materials, even when steel reinforcement is used. However, tailorable ECC materials with inherent tight CW control have been intentionally designed to meet this rigorous requirement (see section 1.3).

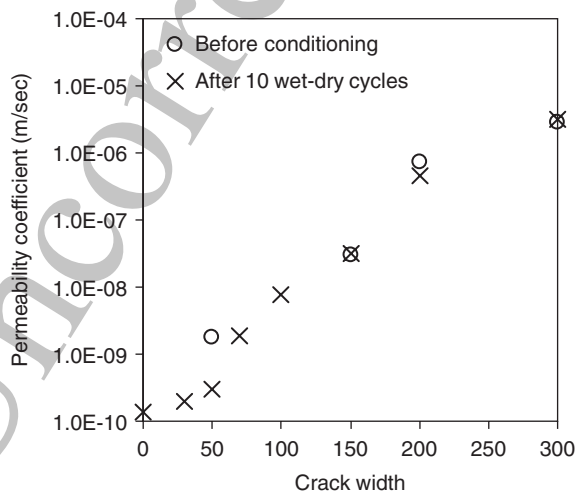

Fig. 6 Permeability coefficient as a function crack width before and after conditioning

2.4 Quality of Self healing in ECC

In this section, the quality of autogenous self healing in ECC is summarized. The ECC material utilized for these studies has a tensile strain capacity of 3% and steady-state CW of 50 μm. The recovery of resonant frequency, mechanical tensile properties, and transport properties (water permeability and chloride diffusivity) were examined under selected environmental conditioning regimes (section 2.2).

2.4.1 Recovery in Dynamic Modulus

Dynamic modulus measurement was used to monitor the rate and extent of self healing. ECC coupon specimens measuring 230 × 76 × 13 mm were prepared and preloaded to different predetermined uniaxial tensile strain levels from 0.3% to 3% at 6 months. On unloading, a small amount of crack closing, 15–20%, was observed depending on the preloading strain magnitude. These specimens were subsequently exposed to wet–dry cycles. Figure 7a and b shows the resonant frequency of ECC specimens with various pre-damage levels (0.3% – 3%) under cyclic wetting and drying CR1 and CR2, respectively. The shaded area indicates the range of resonant frequencies of virgin ECC specimens which had undergone the same cyclic wetting and drying conditioning regime. From these two figures, it can be seen that the resonant frequencies of all preloaded ECC specimens gradually recovers under both conditioning regimes. Ultimately, the resonant frequencies stabilize after 4–5 cycles. These results demonstrate that roughly 4–5 wetting and drying cycles are adequate to engage noticeable self healing of cracked ECC material. Specimens subjected to higher pre-tensioning strains exhibit a lower initial frequency after cracking, due to a larger number of cracks (i.e. damage), and ultimately lower recovery values after wet–dry cycles.

The extent of self healing within preloaded ECC specimens can be evaluated by calculating the ratio of the final resonant frequency after wet–dry cycles to the initial uncracked resonant frequency as depicted in Figure 8. From Figure 8 it can be seen that the resonant frequencies of most specimens approached or even exceeded 100% of their initial resonant frequency when increases due to additional hydration were not considered, the highest of which reaches 110% of the initial frequency. To account for this, the resonant frequencies of virgin uncracked ECC specimens under the same conditioning regimes (10 cycles of CR1 or CR2) were measured. After normalizing the results by taking account of the hydration increase, the resonant frequencies for CR1 tests after preloading were 40–82% of initial, while after wet-dry cycles had regained dynamic modulus 87–100% of initial values. For CR2 conditioning, the resonant frequencies after pre-loading were 31–83% of the initial value and after self healing had stabilized at 77–90% of initial.

Of particular interest is the relation between the extent of self healing and level of strain in the preloaded ECC specimens under CR1. Preloaded testing series with tensile strain of 0.5% exhibited a reduction in resonant frequency of only 18%, while

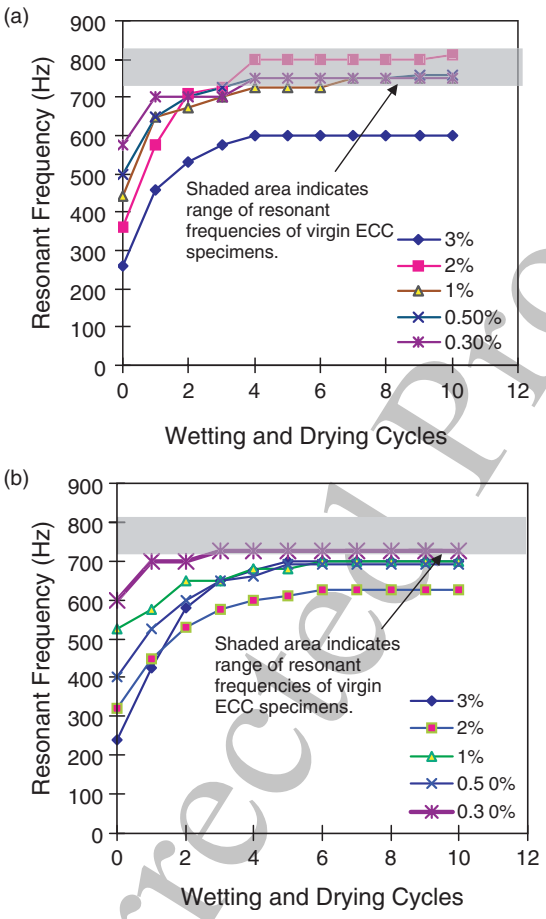

Fig. 7 Self healing rate of ECC under cyclic wetting and drying: (**a**) Resonant frequency recovery under CR1 (water/air cycle); (**b**) Resonant frequency recovery under CR2 (water/hot air cycle)

those preloaded to 3% strain showed an initial reduction of 60%. Self healing in 0.5% strained specimens showed rebounded resonant frequencies back to 100% of initial values, while specimens preloaded to 3% strain returned to only 87% of initial frequencies. This phenomenon is captured in Figure 9, which highlights the rebound in resonant frequency versus number of cracks within the ECC specimen. As the number of cracks grows, the rebound in resonant frequency due to self healing grows. However, the ultimate self healed condition may not be as complete as in specimens strained to a lower deformation. This is likely due to the presence of a greater number of cracks within the highly strained specimens. Within self healed ECC specimens, the material which heals the cracks is typically much weaker than the surrounding mortar matrix. With an increasing number of cracks, while the opportunity for a greater amount of healing exists, the likelihood of healing all these cracks to a level

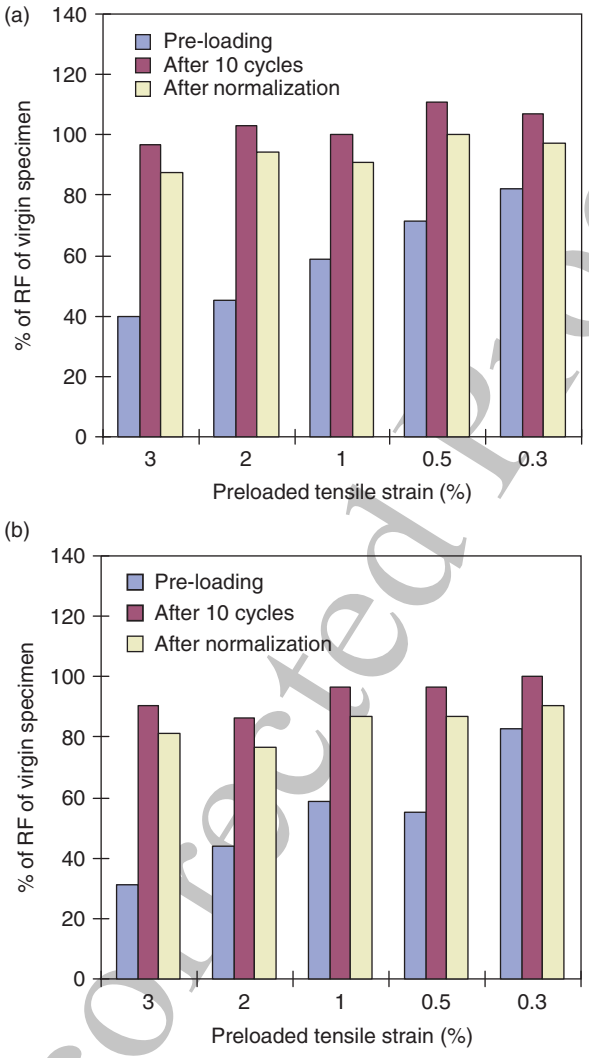

Fig. 8 Extent of self healing in ECC under cyclic wetting and drying: (**a**) Extent of self healing in ECC under CR1 (water/air cycle); (**b**) Extent of self healing in ECC under CR2 (water/hot air cycle)

similar to the uncracked state drops. Therefore, the accompanying reduction in ultimate self healing state (i.e. final resonant frequency) with an increase in strain capacity is not altogether surprising.

In addition to this, a noticeable difference exists in the extent of self healing within specimens subjected to CR1 and CR2. This is most evident in Figure 8. While most specimens subjected to CR1 recovered their full initial dynamic modulus, those subjected to CR2 did not. This may be due to the temperature effects associated with

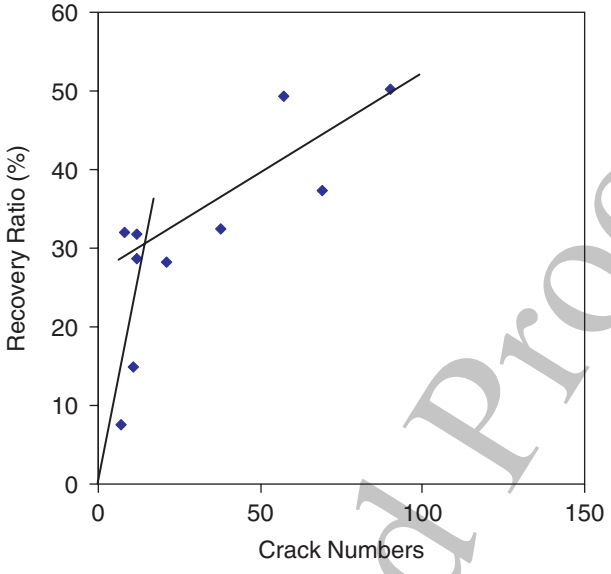

Fig. 9 Rebound in resonant frequency versus number of cracks within the ECC specimen

the CR2 conditioning regime. After submersion in water at 20°C, these specimens are then oven dried at 55°C. During this process, moisture escapes from the specimens through evaporation. As the water evaporates, steam pressure builds up within the pores, resulting in internal damage and potential microcracking. This additional damage which takes place during the self healing process, coupled with the initial damage due to cracking, may handicap CR2 specimens and ultimately result in lower amounts of self healing when compared to CR1 specimens.

2.4.2 Recovery of Tensile Properties

Uniaxial tensile test was conducted to measure the tensile mechanical properties of ECC specimens after self healing. ECC specimens measuring $230 \times 76 \times 13$ mm were prepared and preloaded to different predetermined strain levels from 0.3% to 3% at 6 months. After straining and unloading, the cracked specimens were exposed to 10 wet–dry cycles (CR1 or CR2). Uniaxial tensile tests were conducted again in the rehealed specimens. In the stress–strain curve of the reloading stage, the permanent residual strain introduced in the preloading stage is not accounted for.

Figures 10 and 11 show the preloading tensile stress–strain curves of ECC specimens as well as the reloading tensile stress–strain curves of rehealed ECC specimens after conditioning cycles CR1 and CR2, respectively. For the CR1 test series, the tensile strain capacity after self healing for these specimens ranges from 1.7% to 3.1%. The tensile strain after self healing for CR2 specimens ranges from 0.8% to

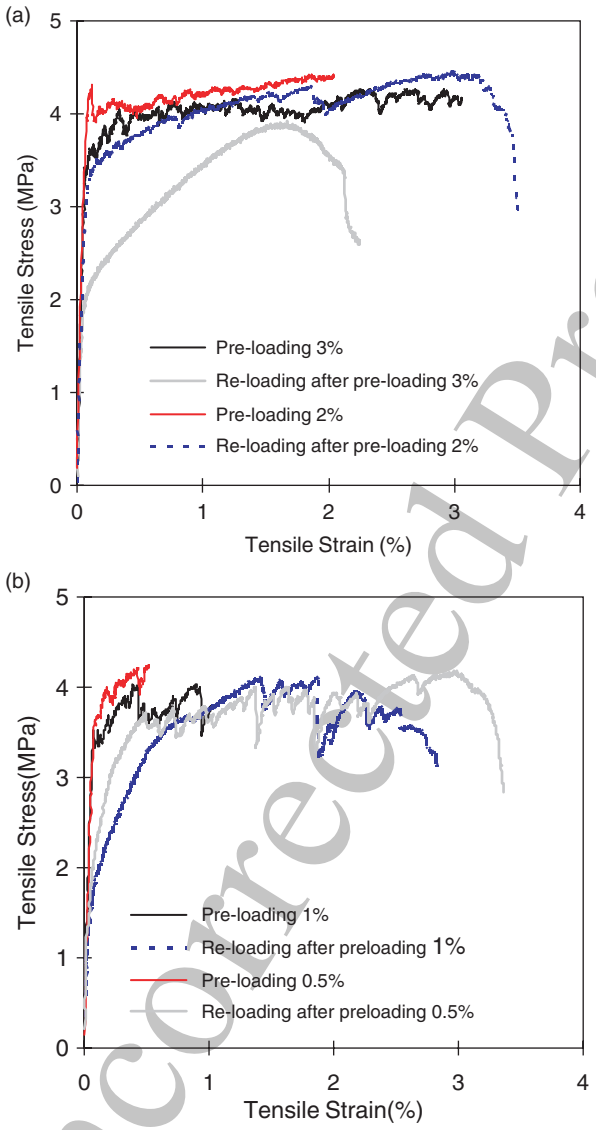

Fig. 10 Preloading and reloading after 10 CR1 (water/air) cycles tensile stress–strain relations of ECC specimens: (**a**) Specimen with preloading above 1%; (**b**) Specimens with preloading to or below 1%

2.2%, slightly lower than that of CR1. However, the ultimate strength after self healing for the CR2 specimens is higher than that of CR1 specimens. The difference of the ultimate tensile strength and tensile strain capacity after self healing can likely be attributed to the different cyclic conditioning regimes. Recall that specimens

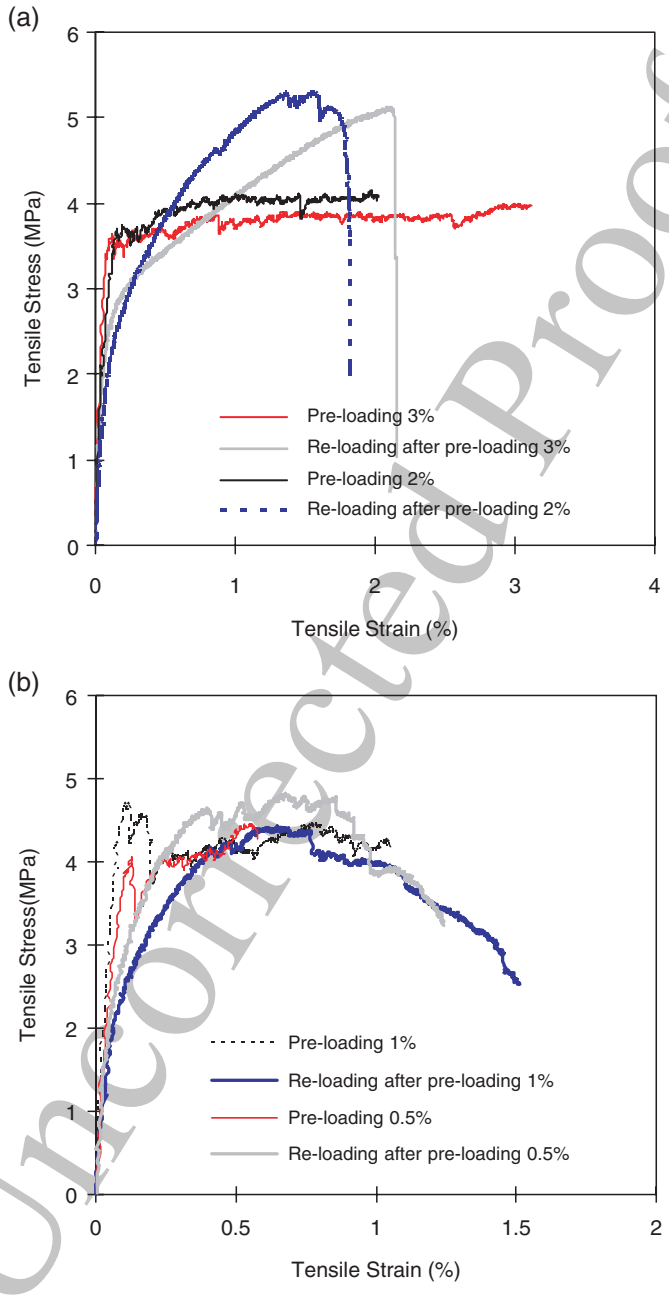

Fig. 11 Preloading and reloading after 10 CR2 (water/hot air) cycles tensile stress–strain relations of ECC specimens: (**a**) Specimen with preloading above 1%; (**b**) Specimen with preloading to or below 1%

subjected to CR2 were submersed in water and then dried in air at 55°C. With this temperature increase, the moisture in the specimens will migrate out and may result in a process similar to steam curing. Therefore, hydration of unreacted cement and fly ash will be accelerated, leading to an increased strength of the ECC matrix and fiber/matrix interfacial bonding (due to a strong hydrophilic nature of PVA fiber). The increase of interface bond strength leads to the increase of fiber bridging strength, and therefore higher composite ultimate tensile strength in CR2. On the other hand, the increase of matrix cracking strength prevents crack initiating and propagation from multiple defect sites and strong interfacial bonding increases the tendency of fiber rupture. Both mechanisms are known [17] to cause a negative impact on the development of multiple microcracking, and therefore lower tensile ductility in CR2 as a consequence.

Figure 12 shows the tensile stress–strain curves of ECC specimens which have been preloaded to 2% or 3% strain levels, then unloaded, and immediately reloaded. Thus these specimens have no opportunity to undergo any self healing. As expected, there is a remarkable difference in stiffness between the virgin specimen and the preloaded specimen under tension. This is due to the reopening of cracks within preloaded specimen during reloading. The opening of these cracks offers very little resistance to load, as the crack simply opens to its previous CW. Once these cracks are completely opened; however, the load capacity resumes, and further tensile straining of the intact material (between adjacent microcracks) can take place. By comparing the material stiffness of self healed specimens in Figures 10 and 11 with that shown for the preloaded specimens without self healing in Figure 12, it can be seen that a significant recovery of the stiffness of ECC specimens after self healing (Figure 13).

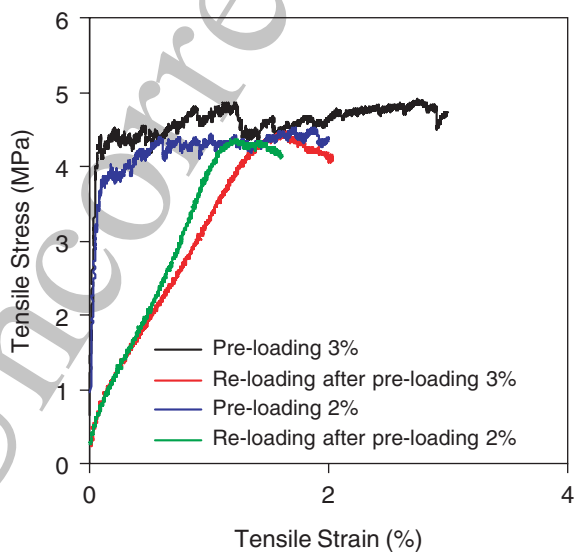

Fig. 12 Preloading and reloading without self healing tensile stress–strain curve of ECC specimens

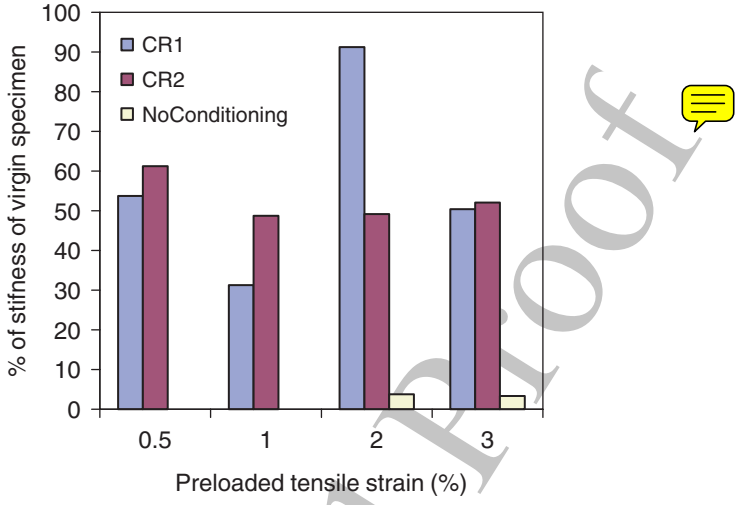

Fig. 13 Stiffness recovery of ECC under different conditioning regime

In other words, self healing of ECC material can result not only in possible sealing of cracks as shown by others, but in true rehabilitation of tensile mechanical properties, in this case the stiffness of the material under tensile load.

This finding is also supported by the rebound of resonant frequency seen in the self healed ECC specimens. As outlined in ASTM C215, resonant frequency is directly related to the dynamic modulus, or stiffness, of a material. The self healing shown through resonant frequency measurements demonstrates the same self healing as that shown in the stiffness gain of tensile coupons. This congruent finding can be used to validate the results of both test series, resonant frequency, and direct tension testing.

Figure 14 shows an ECC specimen subjected to tensile loading after undergoing self healing through the CR1 conditioning regime. This specimen was initially subjected to 2% strain before being exposed to wet–dry cycles. The distinctive white residue, characteristic of crystallization of calcium carbonate crystals, is abundant within the crack and near the crack face on the specimen surface. Further, it can be seen that the majority of cracks which form in self healed specimens tend to follow previous crack lines and propagate through the self healed material. This is not surprising due to the relatively weak nature of calcium carbonate crystals in comparison to hydrated cementitious matrix. The lower first cracking strength in the rehealed specimen (Figures 10 and 11) is also attributed to that the first crack in the rehealed specimen under tension starts from the self healed material (calcium carbonate) which has a lower strength compared to adjacent hydrated cementitious matrix.

However, this is not always the case. As can be seen in Figures 15 and 16, new cracks and crack paths have been observed to form adjacent to previously self healed cracks which now show little or no new cracking. The possibility of this event depends heavily upon the cracking properties of the matrix adjacent to the self

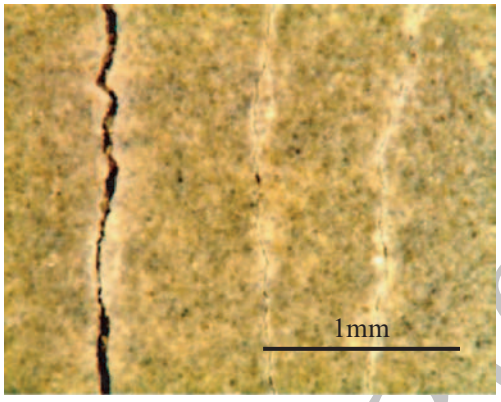

Fig. 14 Cracks through self healed material due to reloading after wet–dry cycles

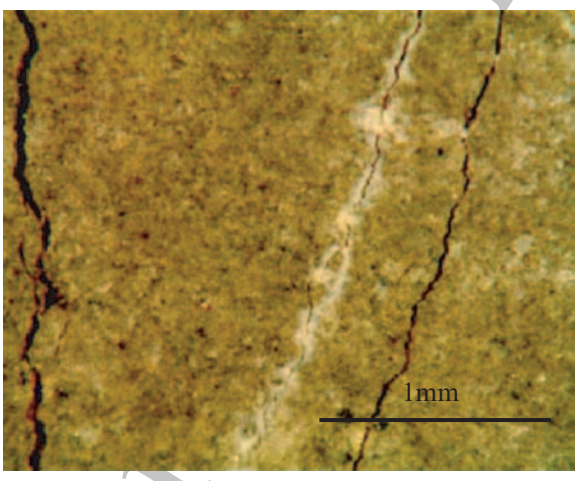

Fig. 15 Cracks through virgin ECC material adjacent to a self healed crack held tight by self healing material

healing, and the quality of the self healing material itself. However, this phenomenon serves as testament to the real possibilities of mechanical self healing within ECC material.

2.4.3 Recovery of Transport Property

Reduction of permeability coefficient in cracked ECC due to self healing

Permeability specimens were cast into coupon plates with cross-sectional dimensions of 13 × 76 mm and 305 mm in length. The specimens were preloaded to the

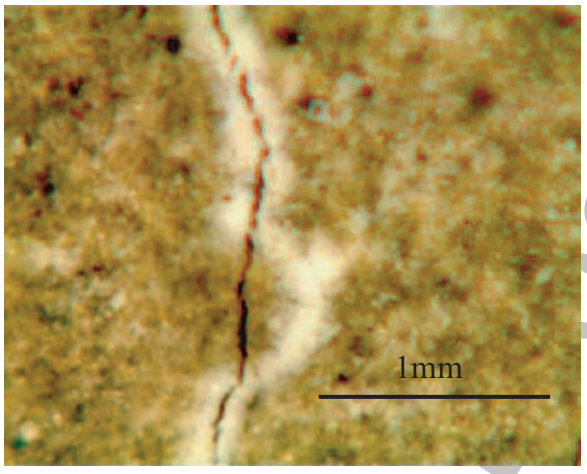

Fig. 16 Meandering new crack path partially deviating from previously self healed crack

predetermined tensile strain. Prior to the permeability testing (CR3), ECC specimens were kept in water for 14 days to ensure complete water saturation. The edges of the coupon specimen were sealed with epoxy to facilitate unidirectional flow through the cross section. Due to the length of time associated with this type of testing, CW permeability measurements were performed in the unloaded state.

Figure 17 shows the rate of permeation through the ECC specimens dropped drastically from the initial values until asymptotically reaching the recorded value, even though the CWs during permeability testing do not change. This phenomenon can be partially attributed to achieving complete saturation and further densification of the matrix throughout the testing period. However, ECC specimens were saturated in water for 14 days prior to permeability testing at an age of 28 days. By the time of testing, the specimens should have been nearly, if not completely, saturated and continuing to undergo little matrix hydration.

Throughout the course of permeability testing, a white residue formed within the cracks and on the surface of the specimens near the cracks. These formations are shown in Figure 18. Figure 18a shows a saturated ECC specimen immediately prior to the beginning of permeability testing, while Figure 18b shows the same specimen after permeability testing. The white residue forms both within the cracks, and within the pores on the surface of the ECC specimen. The effect of self healing of cracks on permeability has been investigated by other researchers [1], and may be significant in the permeability determination of cracked ECC. This can be attributed primarily to the large binder content and relatively low water to binder ratio within the ECC mixture. The presence of significant amounts of unhydrated binders allows for autogeneous healing of the cracks when exposed to water. This mechanism is particularly evident in cracked ECC material due to the small CWs which facilitate self healing. However, this phenomenon is not observed while cracked ECC specimens are

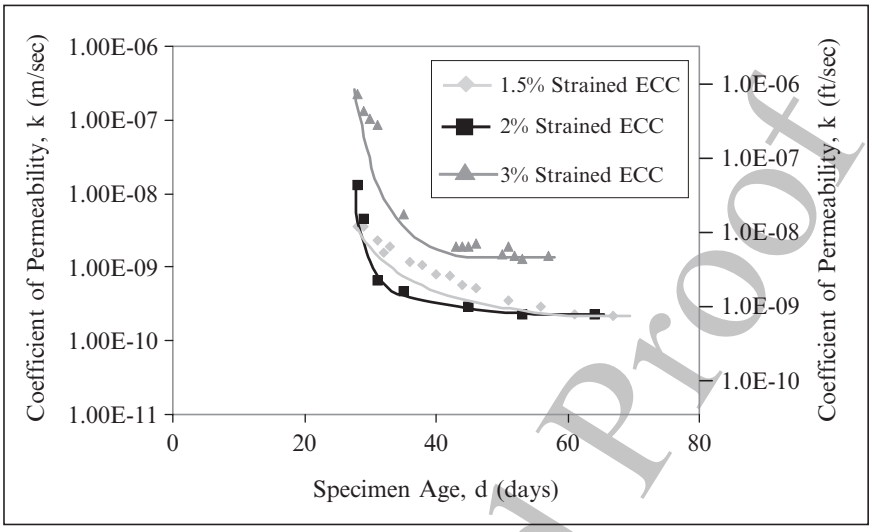

Fig. 17 Development of permeability for ECC strain to 1.5%, 2%, and 3%

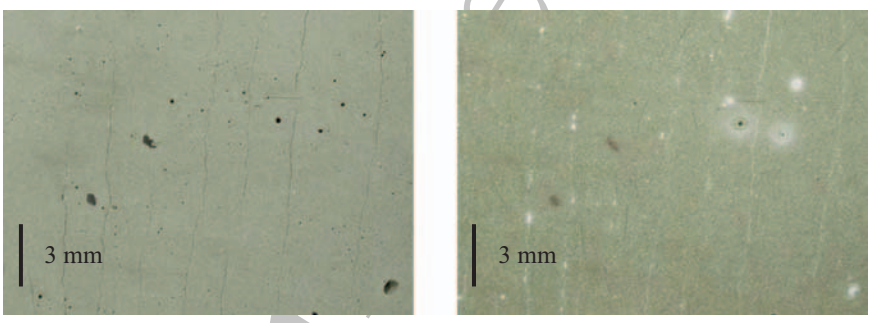

Fig. 18 Appearance of ECC permeability speciemens (**a**) before permeability testing, and (**b**) after permeability testing

simply saturated in water (CR5). During the 14 days of saturation prior to permeability testing, cracked ECC specimens showed no signs of autogeneous healing of the cracks. After only 3 days in the permeability testing apparatus, evidence of self healing became apparent. A similar phenomenon was also seen when cracked ECC specimens were partially submerged in water. Crack healing was only exhibited near the surface of the water, while no healing was observed above or below the water surface.

Surface chemical analysis (XEDS) of the self healing ECC specimens using an environmental scanning electron microscope (ESEM) show that the crystals forming within the cracks, and on the surface adjacent to the cracks, are hydrated cement

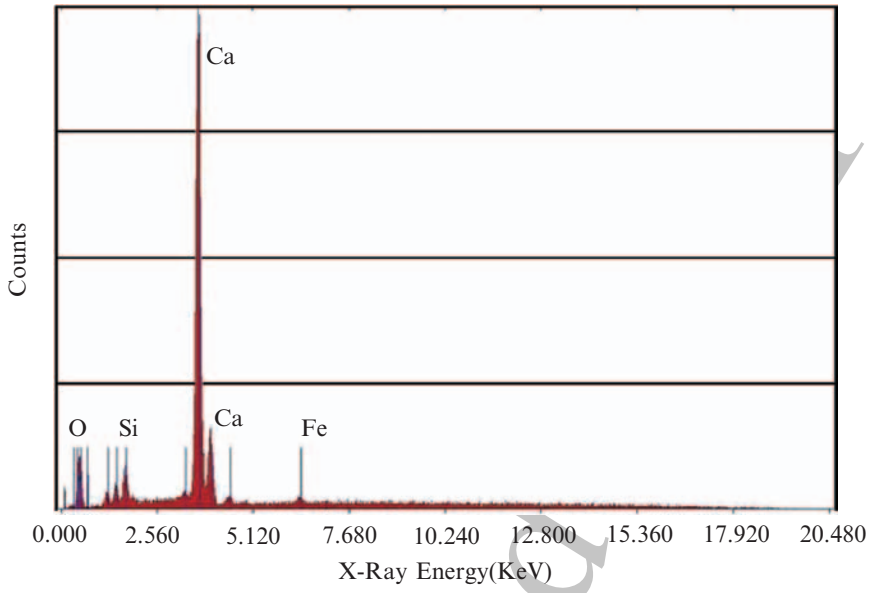

Fig. 19 ESEM surface chemical composition analysis (XEDS) of self healing crack formations

products, primarily calcium carbonate (Figure 19). These crystal formations within the self healed cracks are shown in Figure 20. To facilitate healing of the cracks, and promote formation of calcium carbonate, a flow of water containing carbonates or bicarbonates must be present. Within the permeability testing, these carbonates were introduced by the dissolution of CO_2 in air into the water which flows through the specimens. In the case of the partially submerged specimens, the small amount of carbon dioxide dissolved at the water surface was sufficient to cause limited self healing at that location. However, in the absence of this constant carbonate supply, as in the saturation tanks prior to permeability testing, no self healing of the ECC microcracks can occur. Ultimately, the formation of these crystals slows the rate of permeation through the cracked composite and further reduces the permeability coefficient.

Reduction of diffusion coefficient in ECC due to self healing

Autogenous self healing was also observed in an attempt to measure the diffusion coefficient of damage ECC specimen by means of the chloride-ponding test. Salt-ponding test in accordance with AASHTO T259–80 (Standard Method of Test for Resistance of Concrete to Chloride Ion Penetration) was conducted to evaluate another transport property, effective diffusion coefficient, of material either virgin (uncracked), preloaded (damaged/cracked), or rehealed specimen. After ponding for a certain period (30 days for the preloaded specimen and 90 days for the virgin specimen), the salt solution was removed from the prism surface. Powder samples were

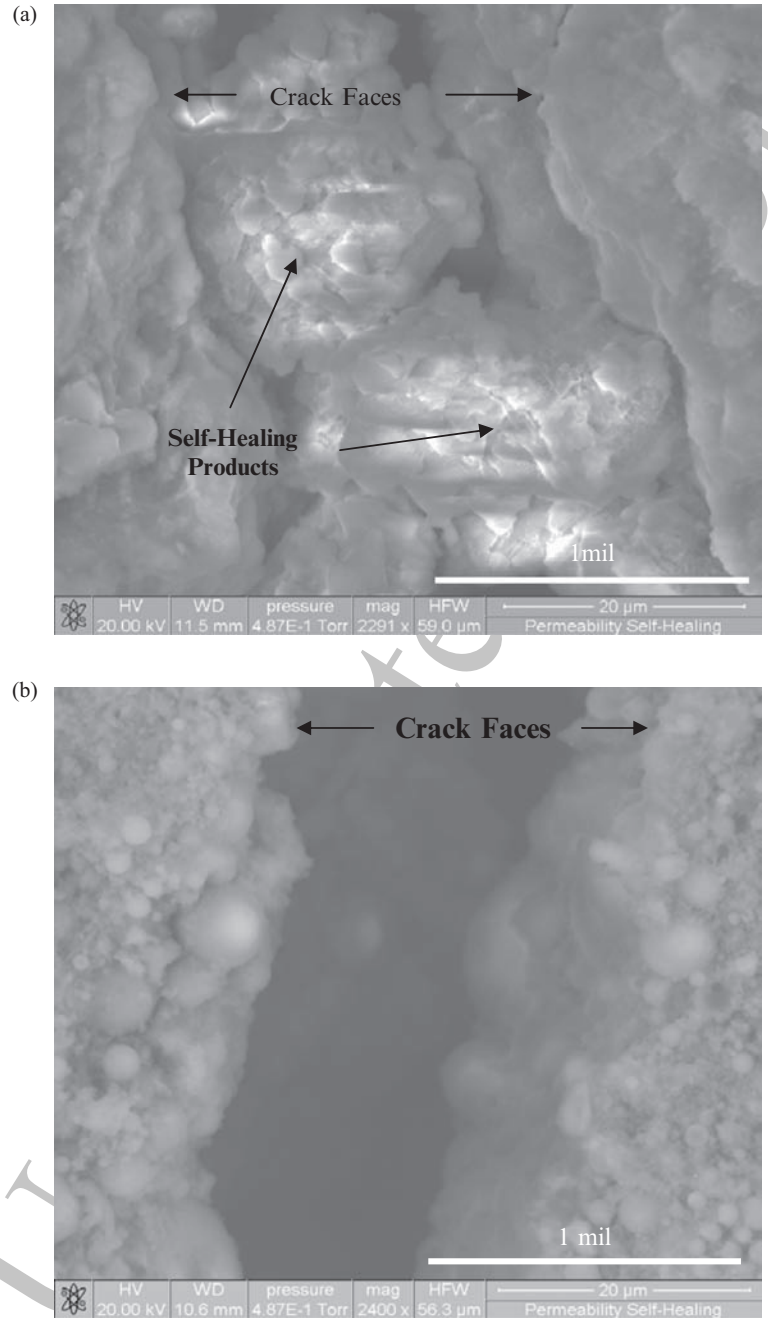

Fig. 20 Morphology of crack within ECC specimen from ESEM: (**a**) Autogenous self healing crystalline formations in ECC crack after permebaility testing; (**b**) ECC crack before permeability testing

taken from the specimen for chloride analysis at various depths from the exposed surface. Total chloride (acid-soluble) content by weight of material at each sampling point was examined according to AASHTO T 260–97 (Standard Method of Test for Sampling and Testing for Chloride Ion in Concrete and Concrete Raw Materials).

The chloride profiles were then input into statistical and curve-fitting software. Equation 3, Crank's solution to Fick's second law, was fitted to the data. The regression analysis yielded the values of the effective diffusion coefficient (D_e) and surface chloride concentration (C_s) for the specimen.

$$C(x,t) = C_s\left[1 - erf\left(\frac{x}{2\sqrt{D_e t}}\right)\right] \tag{3}$$

where

$C(x,t)$ = chloride concentration at time t at depth x
C_s = surface chloride concentration
D_e = effective chloride diffusion coefficient
t = exposure time
$erf()$ = error function

In conducting the ponding test, ECC prism specimens measuring 356 × 76 × 51 mm were prepared. In addition to ECC material, mortar prisms were also tested for comparison purpose. The mortar prisms were reinforced with three levels of steel mesh in order to preload the specimen to a predetermined deformation. At the age of 28 days, prisms surface were abraded using a steel brush as required by AASHTO T259– 80. The prisms were preloaded using four-point bending test to a predetermined deformation. The ponding test was then performed in the unloaded state. Plexiglass was used around the side surfaces of the prism to build an embankment for holding chloride solution on the exposed surface of prisms. At 29 days of age, a 3% of NaCl solution was ponded on the cracked surface of prisms. In order to retard the evaporation of solution, aluminum plates were used to cover the top surface of the specimens.

Table 3 shows the preloaded beam deformation (BD) value, their corresponding average CWs, depths and number of cracks for prism specimens. Two virgin prisms from each mixture were tested without preloading for control purpose. Note that preloading of the mortar beams were limited to 0.83 mm due to the large CW (∼400 μm) and crack depth 70 mm generated in these specimens. In the ECC specimens, the CW remains at about 50 μm even after BD at 2 mm. The crack length becomes impossible to measure accurately due to the tight CW. Table 3 also shows the corresponding number of cracks for prism specimens at each BD value. As seen from this table, when the deformation applied to the prism specimens is increased, the number of cracks on ECC is clearly increased but the CW did not change for the different deformation values. Micromechanically designed ECC changes the cracking behavior from one crack with large width to multiple smaller cracks as described in section 1.3.

Table 3 Crack widths, numbers, and depths of preloaded ECC and mortar prisms

Material	Beam Deformation (mm)	Average Crack Width (μm)	Crack Depth (mm)	Crack Number
Mortar	0.5	~ 50	20	1
	0.7	~ 150	36	1
	0.8	~ 300	55	1
	0.83	~ 400	70	1
ECC	0.5	~ 0	N/A	0
	1.0	~ 50	N/A	15
	1.5	~ 50	N/A	21
	2.0	~ 50	N/A	35

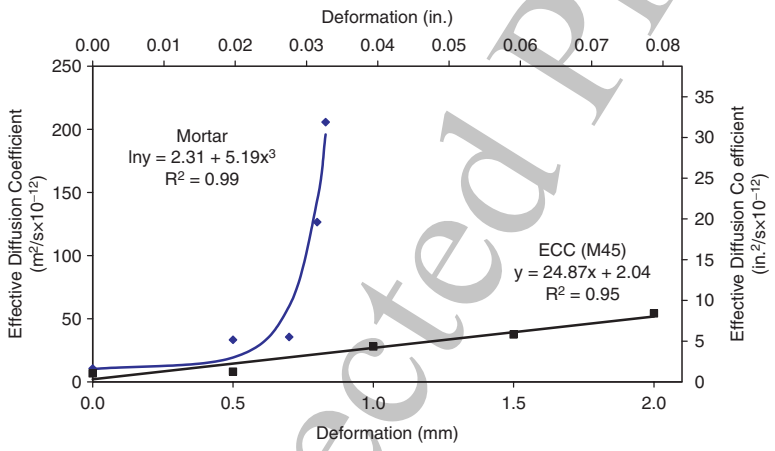

Fig. 21 Diffusion coefficient versus preloading deformation level for ECC and mortar

Figure 21 shows the relationship between the effective diffusion coefficient of chloride ions and the BD level, for mortar and ECC specimens. Despite the same or higher magnitude of imposed overall deformation and higher crack density, the ECC specimens reveal an effective diffusion coefficient considerably lower than that of the reinforced mortar because of the tight CW control. Especially for the higher deformation level, the effective diffusion coefficient of mortar increased exponentially with BD. The effective diffusion coefficient of ECC; however, increased linearly with the imposed deformation value, because the number of microcracks on the tensile surface of ECC is proportional to the imposed BD. The total chloride concentration profiles perpendicular to the crack path indicate no significant chloride penetration even at large imposed deformation (2 mm) for ECC specimens.

The reason for the relatively low diffusion coefficient of cracked ECC specimens is not only due to the tight CW but also the presence of self healing of the microcracks. The self healing of cracks becomes prominent when CW is small. In the case of precracked ECC prisms exposed to salt solution, a distinct white deposit was visible over the crack surface at the end of 1-month exposure period (Figure 22). These

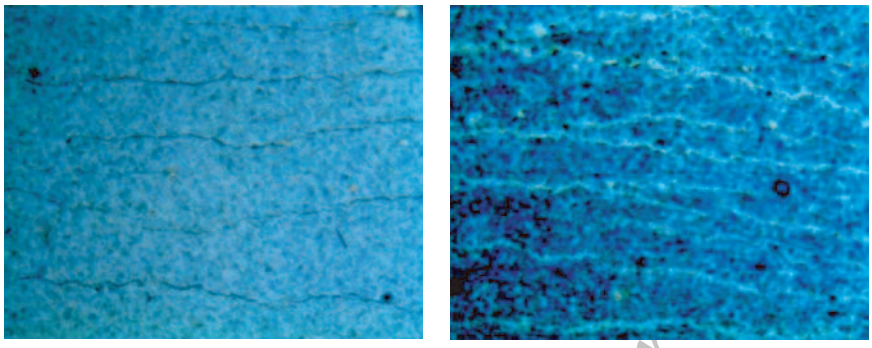

(a) (b)

Fig. 22 Self healing products in ECC microcracks (**a**) before, and (**b**) after salt-ponding test at 30 days exposure

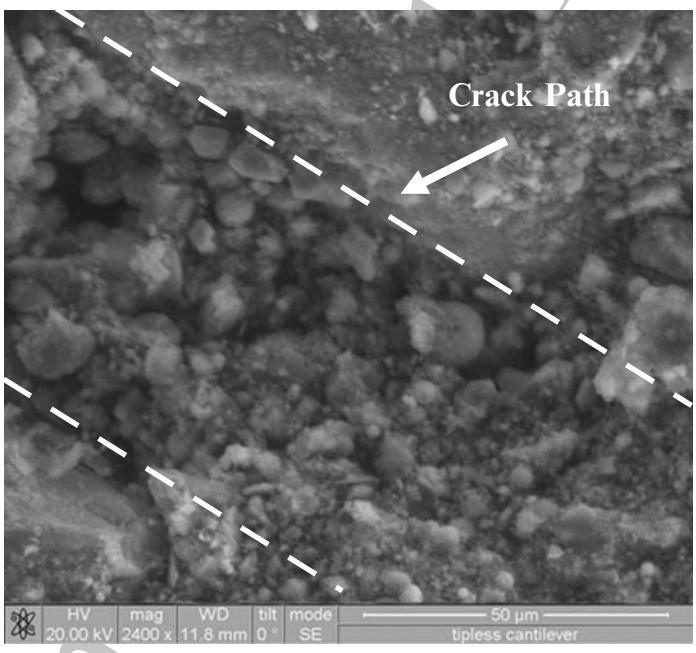

Fig. 23 ESEM micrograph of rehydration products in a self healed crack

deposits were most probably caused by efflorescence due to leaching of calcium hydroxide (CH) into cracks and due to the presence of NaCl ion in solution. This white deposit on the crack surface easily blocked the flow path due to smaller CW of ECC. An ESEM observation of the fractured surface of ECC across a healed crack is shown in Figure 23. The present ESEM observations show that most of the products seen in the cracks were newly formed C-S-H gels. CH and deposition of salts in

the crack path were also observed. These observations indicate that microcracks of ECC exposed to NaCl solution healed completely after exposure for 30 days to NaCl solution. This can be attributed primarily to the large fly ash content and relatively low water to binder ratio within the ECC mixture. The continued pozzolanic activity of fly ash is responsible for the self healing of the crack which reduces the ingress of the chloride ions.

3 Conclusions

From the resonant frequency (after wet–dry cycle exposure) and permeability measurements, it appears that a maximum CW of 50 μm is necessary to achieve full recovery of mechanical and transport properties in ECC material. Between 50 and 150 μm, partial recovery can be attained.

Under both water/air cycle and water/hot air cycle environments, a recovery of resonant frequent above 80% is achievable for ECC specimens pretensioned to as much as 3% strain. Most self healing appears to occur within the first 4–5 cycles. Under these same conditions, 100% recovery of the initial elastic modulus can be attained. Further the original ultimate tensile strength and strain capacity are retained after rehealing. However, the first crack strength may be lower especially for those specimens with large prestraining, probably due to the weakness in some partially healed crack planes. In this case, crack formation upon reloading will likely take place where a partially healed crack is present. For specimens with lower amount of prestraining, complete rehealing occurs so that new cracks are observed near rehealed cracks upon reloading. This is in spite of the fact that the products formed inside the cracks are calcites known to be relatively weak. It is possible that the bridging fibers serve as nucleation sites for the calcite crystals while simultaneously act as reinforcements. Further study on the details of reheal product formation process is needed.

Both transport properties, permeability, and chloride diffusion, showed a decrease over time. Precracked ECC specimens exposed to water flow in the permeability experiments showed rehealing through calcite formation, while precracked ECC specimens exposed to saltwater ponding showed rehealing through CH formation.

From these studies, it becomes evident that self healing both in the mechanical and transport sense is present in ECC. The deliberate engineering of ECC to maintain extremely tight CW even under large imposed deformation as carried out in these experiments, is largely responsible for the quality of autogenous self healing in this material. The low water/cement ratio in addition to the large amount of fly ash also aids in promoting self healing via continued hydration and pozzolanic activities. These activities are expected to extend indefinitely since unhydrated cement and unreacted fly ash in concrete materials are known to have a long shelf life.

Similar to all concrete materials, the micro-reservoirs of unhydrated cement and unreacted fly ash in ECC ensures self healing to be pervasive throughout a structure.

The very act of creating a crack is expected to provide advective–diffusive forces that drives free calcium ions towards the crack surface and enhances the tendency to form rehealing products in the crack in the presence of water and dissolved CO_2. This suggests that chemicals are always intrinsically present where it is needed for self healing. (External water and CO_2 in air is expected to be plentiful especially for transportation infrastructure.) Unlike other concrete materials, ECC has the ability to self-control CW down to the 50 μm range and below, which drastically enhances the reliability of self healing, as demonstrated in the test results described for a variety of exposure environments in this article. Also demonstrated is the quality of rehealing especially for ECC specimens preloaded to below 1% tensile strain. Recovery of mechanical and transport properties reaching 80% or above is evident. Additional research is needed to confirm the repeatability of the self healing functionality in ECC subjected to tensile load cycles.

Acknowledgments

This work has drawn upon a body of research with participations from M. Lepech, M. Sahmaran, and Y. Yang. Their contributions are greatly appreciated. The authors would also like to acknowledge helpful comments by K. van Brugel and E. Schlangen at Delft University, and by K. Maekawa at University of Tokyo. This research was funded through an NSF MUSES Biocomplexity Program Grant (Nos. CMS-0223971 and CMS-0329416). MUSES (Materials Use: Science, Engineering, and Society) support projects that study the reduction of adverse human impact on the total interactive system of resource use, the design and synthesis of new materials with environmentally benign impacts on biocomplex systems, as well as the maximization of efficient use of materials throughout their life cycles.

References

1. Edvardsen C (1999) Water permeability and autogenous healing of cracks in concrete. ACI Mater J 96:448–455
2. Reinhardt H, Joos M (2003) Permeability and self-healing of cracked concrete as a function of temperature and crack width. J cement concrete Res 33:981–985
3. Pimienta P, Chanvillard G (2004) Retention of the mechanical performances of Ductal specimens kept in various aggressive environments. Fib Symposium.
4. Granger S, Pijaudier-Cabot G, Loukili A (2007) Mechanical behavior of self-healed Ultra High Performance Concrete: from experimental evidence to modeling. Accepted for publication in Proc. FRAMCOS 6. Catalina, Italy
5. Ter Heidi N, Schlangen E, van Breugel K (2006) Experimental study of crack healing of early age cracks. In: Proceedings of Knud Hojgaard Conference on advanced cement-based materials: research and teaching. Lyngby, Denmark
6. White SR, Sottos NR, Geubelle PH, Moore JS, Kessler MR, Sriram SR, Brown EN, Viswanathan S (2001) Autonomic healing of polymer composites. Nature 409:794–797

7. Kessler MK, Sottos NR, White SR (2003) Self-healing structural composite material. Compos Part A: Appl Sci Manuf 34(8):743–753
8. Dry C (1994) Matrix crack repair and filling using active and passive model for smart time release of chemicals from fibers into cement matrixes. J Smart Mater Struct 118–123
9. Dry C (1996) Procedures developed for self-repair of polymer matrix composite materials. Compos Struct 35:236–269
10. Li VC, Lim YM, Chan Y (1998) Feasibility study of a passive smart self-healing cementitious composite. Compos Part B 29B:819–827
11. Dry C (1996) Release of smart chemicals for the in-service repair of bridges and roadways. In: Proceedings of the Symposium on Smart Materials, Structures and MEMS
12. Lee JY, Buxton GA, Balazs AC (2004) Using nanoparticles to create self-healing composites. J Chem Phys 121(11):5531–5540
13. Nishiwaki T, Mihashi H, Jang BK, Miura K (2006) Development of self-healing system for concrete with selective healing around crack. J Adv Concrete Techn **4**(2):267–275
14. Bang SS, Galinat JK, Ramakrishnan V (2001) Calcite precipitation induced by polyurethane-immobilized Bacillus pasteurii. Enzyme Microb Tech 28:404–409
15. Rodriguez-Navarro C, Rodriguez-Gallego M, Chekroun KB, Gonzalez-Munoz MT (2003) Conservation of ornamental stone by myxococcus santhus-induced carbonate biomineralization. Appl Environ Microbiol 2182–2193
16. Li VC (2003) On engineered cementitious composites (ECC) – a review of the material and its applications. J Adv Concrete Tech 1(3):215–230
17. Li VC, Wu C, Wang S, Ogawa A, Saito T (2002) Interface tailoring for strain-hardening PVA-ECC. ACI Mater J 99(5):463–472
18. Lepech MDAVCL (2006) Long term durability performance of engineered cementitious composites. Int J Restoration Buildings Monuments 12(2):119–132
19. Kunieda M, Rokugo K (2006) Recent progress on HPFRCC in Japan, required performance and applications. J Adv Concrete Tech 4(1):19–33
20. Clear CA (1985) The effects of autogenous healing upon the leakage of water through cracks in concrete. In: Cement and Concrete Association Technical Report No. 559, p 28
21. Nanayakkara A (2003) Self-healing of cracks in concrete subjected to water pressure. Symposium on new technologies for urban safety of mega cities in Asia. Tokyo, Japan
22. Institute AC (1995) Building code requirements for structural concrete (ACI318–95) and Commentary (ACI318R-95). American Concrete Institute. Detroit, Michigan
23. Joos M (2001) Leaching of concrete under thermal influence. Otto-Graf-J 12:51–68
24. Hannant DJ, Keer JG (1983) Autogenous healing of thin cement based sheets. Cement Concrete Res 13:357–365
25. Farage MCR, Sercombe J, Galle C (2003) Rehydration and microstructure of cement paste after heating at temperatures up to 300°C. J Cement Concrete Res 33:1047–1056
26. Cowie J, Glassert FP (1992) The reaction between cement and natural water containing dissolved carbon dioxide. Adv Cement Res 14(15):119–134
27. Ter Heide N (2005) Crack healing in hydrating concrete. MSc Thesis, TU Delft, The Netherlands
28. Schiessl P, Brauer N (1996) Influence of autogenous healing of cracks on corrosion of reinforcement. In: Proceedings on durability of building materials and components 7
29. Mangat PS, Gurusamy K (1987) Permissible crack widths in steel fiber reinforced marine concrete. J Mater Struct 20:338–347
30. Jacobsen S, Marchand J, Boisvert L (1996) Effect of cracking and healing on chloride transport in OPC concrete. J Cement Concrete Res 26:869–881
31. Jacobsen S, Marchand J, Homain H (1995) SEM observations of the microstructure of frost deteriorated and self-healed concrete. J Cement Concrete Res 25:1781–1790
32. Ismail M, Toumi A, Francois R, Gagne R (2004) Effect of crack opening on local diffusion of chloride inert materials. Cement Concrete Res 34:711–716

33. Aldea C, Song W, Popovics JS, Shah SP (2000) Extent of healing of cracked normal strength concrete. J. Mater Civil Eng 12:92–96
34. Li VC (1997) Engineered cementitious composites – tailored composites through micromechanical modeling. In: Fiber reinforced concrete: present and the future., Canadian Society for Civil Engineering, Montreal, pp 64–97
35. Maalej M, Hashida T, Li VC (1995) Effect of fiber volume fraction on the off-crack plane energy in strain-hardening engineered cementitious composites. J Am Ceramics Soc 78(12):3369–3375
36. Li VC, Chan YW (1994) Determination of interfacial debond mode for fiber reinforced cementitious composites. ASCE J Eng Mech 120(4):707–719
37. Yang E, Li VC (2007) Numerical study on steady-state cracking of composites. Compos Sci Tech 67:151–156
38. Ramm W, Biscoping M (1998) Autogenous healing and reinforcement corrosion of water-penetrated separation cracks in reinforced concrete. J Nucl Eng Des 179:191–200
39. Reinharde H, Jooss M (2003) Permeability and self-healing of cracked concrete as a function of temperature and crack width. J Cement Concrete Res 33:981–985
40. Wang K, Jansen DC, Shah SP, Karr AF (1997) Permeability study of cracked concrete. J Cement Concrete Res 27:381–393
41. Lepech MD, Li VC (2005) Water permeability of cracked cementitious composites. In: ICF 11. Turin, Italy, Paper 4539 of Compendium of Papers CD ROM.
42. Jacobsen S, Sellevold EJ (1996) Self healing of high strength concrete after deterioration by freeze/thaw. J Cement Concrete Res 26:55–62
43. Yang Y, Lepech M, Li VC (2005) Self-healing of ECC under cyclic wetting and drying. In: Proceedings of international workshop on durability of reinforced concrete under combined mechanical and climatic loads. Qingdao, China
44. Cernica JN (1982) Geotechnical engineering. Holt, Reinhart & Winston, New York, pp 97–99
45. Lepech MD (2006) A paradigm for integrated structures and materials design for sustainable transportation infrastructure, PhD Thesis. In: Department of Civil and Environmental Engineering, University of Michigan, Ann Arbor